Planetary and Space Science 88 (2013) 76–85

Contents lists available at ScienceDirect

Planetary and Space Science

journal homepage: www.elsevier.com/locate/pss

Evolution of the Io footprint brightness II: Modeling

S.L.G. Hess [a,*], B. Bonfond [b,c], V. Chantry [d], J.-C. Gérard [c], D. Grodent [c], S. Jacobsen [e,1], A. Radioti [c]

[a] LATMOS, Université Versailles-St Quentin, IPSL/CNRS, 11 Boulevard d'Alembert, 78280 Guyancourt, France
[b] Department of Space Studies, Southwest Research Institute, Boulder, USA
[c] LPAP, Université de Liège, Belgium
[d] ATI, Université de Liège, Belgium
[e] Research and Technology Center Westcoast, University of Kiel, Büsum, Germany

ARTICLE INFO

Article history:
Received 20 December 2012
Received in revised form
5 August 2013
Accepted 8 August 2013
Available online 20 August 2013

Keywords:
Io–Jupiter interaction
Io footprint
Electron acceleration
Alfvén waves

ABSTRACT

The interaction of Io with the Jovian magnetosphere creates the best known and brightest satellite-controlled aurorae in our solar system. These aurorae are generated by the precipitation of electrons, which are accelerated by the Alfvén waves carrying the current between the satellite and the planet. A recent study computed the energy deposited on top of Jupiter's ionosphere due to the electron precipitation and retrieved the correct mean brightness of Io-related aurorae. The model developed in this study takes into account the acceleration mechanism and the Alfvén wave propagation effects. We use the same method to investigate the brightness variation of the different components of the Io footprint as a function of longitude. These observations are discussed in a companion paper. We identify several effects that act together to modulate the footprint brightness such as Alfvén wave reflections, magnetic mirroring of the electrons, the local interaction at Io and kinetic effects close to Jupiter. We identify the effects contributing the most to the modulation of the brightnesses of the three brightest components of the Io footprints: the main and reflected Alfvén wing spots and the transhemispheric electron spot. We show in particular that the modulation of the efficiency of the electron acceleration can be of greater importance than the modulation of the power generated at Io. We reproduce the average modulation of the spot brightnesses and present an extensive discussion of possible explanations for the observed features not reproduced by our model.

1. Introduction

Io is the innermost Galilean satellite of Jupiter. Its interaction with the Jovian magnetosphere generates intense aurorae in the Jovian ionosphere. These emissions are observed from the Infrared (Connerney et al., 1993) to the X-rays (Branduardi-Raymont et al., 2008), but are most studied in the UV domain (Prangé et al., 1996; Clarke et al., 1996), which gives the best spatial and temporal resolutions (Gérard et al., 2006; Bonfond et al., 2009). Because of the non-axisymmetric nature of the magnetic field of Jupiter, this interaction is expected to be modulated by the System III longitude of Io. Such a modulation has indeed been observationally confirmed (Serio and Clarke, 2008; Wannawichian et al., 2010; Bonfond et al., in this issue). The purpose of the present paper is to theoretically investigate this modulation, and to compare our results with the observations discussed in a companion paper (Bonfond et al., in this issue; hereafter Paper I). We first present a short introduction of Io's vicinity and its electromagnetic interaction with Jupiter.

1.1. Basics of the interaction

Io is the most active volcanic body of our solar system, releasing about 1 ton/s of neutral matter in the Jovian magnetosphere. Roughly half of this matter is ionized and remains frozen in the Jovian magnetic field (Bagenal, 1997; Saur et al., 2003; Thomas et al., 2004, and references therein) forming a dense and cold plasma torus concentrated along the centrifugal equator and corotating with Jupiter in 9 h 55 min. Io orbits with a Keplerian period of 42.5 h in the jovigraphic equator. The centrifugal equator is inclined by $\sim 7^\circ$ from Io's orbital plane, intersecting it at the $\sim 22^\circ$ and $\sim 202^\circ$ System III longitudes (Schneider and Trauger, 1995).

The motion of Io relative to the Jovian magnetic field – with a velocity of $V_{Io} = 57$ km/s – and the perturbation of the plasma flow around Io generate an electric field ($E_{Io} = -V_{Io} \times B$), which in turn induces a current (J) (Goldreich and Lynden-Bell, 1969). Due to the short (< 1 minute) duration of the satellite–magnetosphere

* Corresponding author. Tel.: +33 1 80 28 50 63.
E-mail address: sebastien.hess@latmos.ipsl.fr (S.L.G. Hess).
[1] Formerly at: Institut für Geophysik und Meteorologie, Universität zu Köln, Germany.

0032-0633/$ - see front matter © 2013 Elsevier Ltd. All rights reserved.
http://dx.doi.org/10.1016/j.pss.2013.08.005

interactions, the current is not in steady-state but mostly transient (Neubauer, 1980; Goertz, 1983; Hess et al., 2011c). In this case, the current is essentially carried by an Alfvén wave packet propagating at the Alfvén velocity (V_a) toward Jupiter's ionosphere, where the current system finally closes. However, Alfvén waves are partially reflected on the torus borders (Gurnett and Goertz, 1981) due to strong gradients of the plasma density affecting the Alfvén velocity (V_a):

$$V_a = \sqrt{\frac{B^2}{\mu_0 \rho}}, \tag{1}$$

where B is the magnetic field strength, *rho* the plasma density and μ_0 the vacuum permittivity. Upon reflection, a fraction of the wave and thus a part of the current are reflected back in the torus. Hence, the current directly reaching Jupiter is smaller than the one generated at Io. The Alfvén travel time from Io to Jupiter is longer than the time it takes for a magnetic field line to pass Io. As a consequence, remote conductances – e.g. the Jovian ionosphere conductance – do not impact the current generated at Io, and the current can be deduced from the electric field across Io and the height-integrated Alfvén conductance (Σ_A) (Neubauer, 1980; Goertz, 1983):

$$J = 4E_{Io}R_{Io}\Sigma_A \simeq 4V_{Io}R_{Io}\sqrt{\frac{\rho}{\mu_0}} \text{ per hemisphere.} \tag{2}$$

Note that the current expression depends only on local values, indicated by the $_{Io}$ subscript. Every term in the current formula remains constant, except for the plasma density. Since Io's orbit does not lie in the plasma torus plane, the value of the density at Io varies with Io's longitude (λ_{Io}), reaching a maximum where the Io orbit and plasma torus planes intersect (i.e. at $\lambda_{Io} \simeq 110^\circ$ and 290° according to Schneider and Trauger, 1995).

Close to Jupiter, the convergence of the magnetic field lines forces the Alfvén perpendicular wavelengths toward small values, close to that of the electron inertial length. In this case, a parallel electric field appears due to kinetic effects and accelerates electrons (Lysak and Song, 2003; Swift, 2007; Hess et al., 2010a). Part of these electrons precipitate in the Jovian atmosphere and generate aurorae by collision with thermospheric neutrals. The interaction of Io with the Jovian magnetosphere generates the brightest satellite-related auroral emissions of the solar system, fed by the large amount of power radiated by Io:

$$P_w = 2E_{Io}R_{Io}J \simeq 8V_{Io}^2R_{Io}^2B_{Io}\sqrt{\frac{\rho}{\mu_0}} \text{ per hemisphere.} \tag{3}$$

1.2. Basics of the observations

Io auroral footprints have a complex substructure. They are composed of a Main Alfvén Wing (MAW) spot located where the Alfvén wing reaches the Jovian ionosphere and of a Transhemispheric Electron Beam (TEB) spot (Bonfond et al., 2008), both of which are traces of the electron acceleration by Alfvén waves (Swift, 2007; Hess et al., 2010a) that accelerate electrons in the planetward and anti-planetward directions. The planetward electrons precipitate on the MAW spot, whereas the anti-planetward electrons precipitate in the opposite hemisphere, powering the TEB spot. Finally, dimmer Reflected Alfvén Wing (RAW) spots and an extended (up to several tens of degrees) tail (Clarke et al., 2002; Gérard et al., 2006; Bonfond et al., 2009) are mostly due to the multiple reflections of the Alfvén waves carrying the current (Gurnett and Goertz, 1981; Goertz, 1983). The relative positions of these spots vary with Io's longitude (Gérard et al., 2006; Bonfond et al., 2009) in accordance with the geometry of the interaction. Depending on the Io position relative to the plasma torus center, an asymmetry appears between the northern and southern Alfvén wings and their respective footprints, affecting the positions of the auroral spots.

The brightness of these spots is also modulated with the longitude of Io (Serio and Clarke, 2008; Wannawichian et al., 2010). The latest and most precise study of the modulation of the Io footprints with the longitude is published in Paper I. In this study, the authors carefully separated the brightness of each spot comprising the Io footprints, and obtained brightness profiles as a function of the longitude of Io. The main results of Paper I are

(1) the determination of the relative brightnesses of the spots;
(2) the brightness of the spots presents a quasi-sinusoidal modulation with an amplitude of about $\pm$ 30% of the average, whose phase is determined by the position of Io relative to the torus center;
(3) all observed spots present a large peak of brightness in a narrow range of longitudes around 110° of Io's longitude; and
(4) the emissions in the southern hemisphere are on average twice as bright as those in the north.

These results are summarized in Figs. 1 and 2 of the present paper, in which crosses represent the energy flux precipitated over each of the observed auroral spots. These fluxes have been computed from the brightness values measured in Paper I. The measured brightnesses have been converted in precipitating energy fluxes

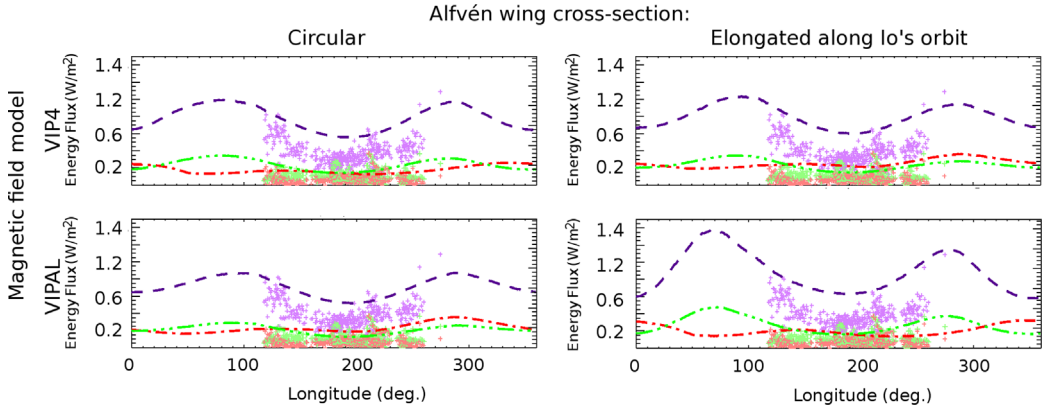

Fig. 1. Modulation of the power emitted by Io northern spots in W m^{-2}. Blue (dashed) line and purple crosses correspond to MAW spot simulated and observed powers, respectively. Red (dot-dashed) line and crosses correspond to TEB spot simulated and observed powers, respectively. Green (dot-dot-dashed) line and crosses correspond to RAW spot simulated and observed powers, respectively. (For interpretation of the references to color in this figure caption, the reader is referred to the web version of this article.)

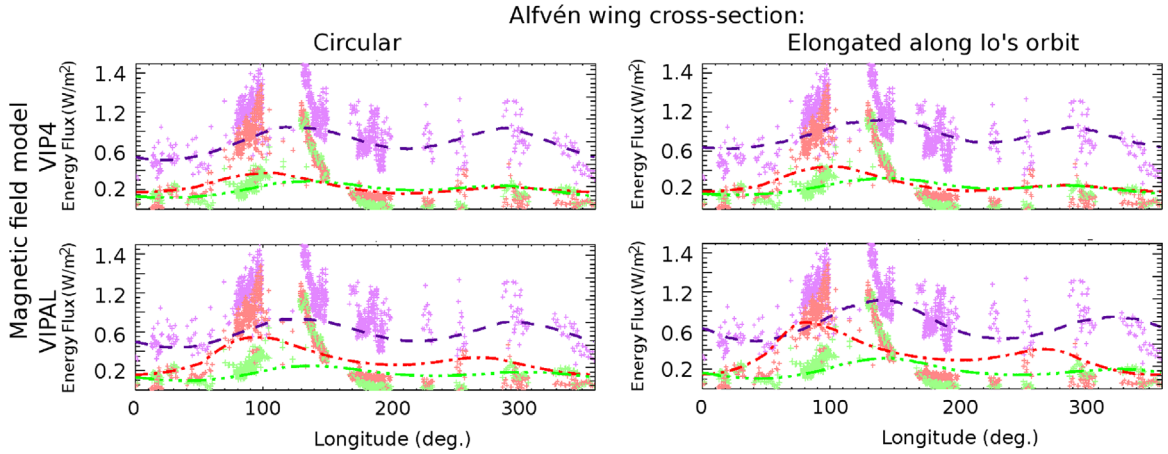

Fig. 2. Modulation of the power emitted by Io southern spots in W m^{-2}. Blue (dashed) line and purple crosses correspond to MAW spot simulated and observed powers, respectively. Red (dot-dashed) line and crosses correspond to TEB spot simulated and observed powers, respectively. Green (dot-dot-dashed) line and crosses correspond to RAW spot simulated and observed powers, respectively. (For interpretation of the references to color in this figure caption, the reader is referred to the web version of this article.)

using the conversion formula determined by Gérard et al. (2006). More details on these results are presented in Paper I.

1.3. Present study

The purpose of the present paper is to investigate theoretically the brightness modulation of the main Io spots as a function of the longitude of Io and to compare it with the observations of Paper I. According to the current observational and theoretical understanding of Io's interaction with the Jovian magnetosphere described above, we propose four possible origins for the observed variations in auroral footprint brightness:

(1) The modulation of the power radiated at Io, which depends only on the magnetic field and plasma density at Io (Eq. (3)).
(2) The reflection of the Alfvén waves on the torus border, which varies as the position of Io in the torus varies with longitude.
(3) The modulation of the efficiency of the electron acceleration, which depends on the magnetic field topology and varies with longitude (Hess et al., 2011b).
(4) The modulation of the magnetic mirroring of the accelerated electrons between the acceleration region and the surface.

These phenomena are carefully discussed in Sections 2–5, respectively. We show that all of them contribute to the modulation of the Io footprint brightness with different relative contributions. We determine that the dominant ones are the modulation of the power radiated at Io and the modulation of the efficiency of the electron acceleration. This permits us to explain two out of the four results of Paper I ($\pm$30% amplitude variation, and relative brightness of the spots within each hemisphere). We are not able to present an explanation for results 3 and 4 of Paper I, since none of the aforementioned phenomena presents the required signature. However, based on the comparison of the longitudinal profiles of all spots, we discuss some possible origins.

2. Modulation of the power generated at Io

The power generated at Io by the satellite interaction with the Jovian magnetosphere is given by Eq. (3). The variables in this equation are only the magnetic field strength and the plasma density at Io.

The magnetic field model most commonly used for the study of the Io–Jupiter interaction is the VIP4 internal magnetic field model (Connerney et al., 1998). It is obtained from the inversion of the magnetic field measurements performed by the Pioneer and Voyager spacecraft and the fit of the Io footpaths. However, the position of the Io footprints as a function of Io longitude has not been taken into account, leading to a large (tens of degrees) inaccuracy on the longitudinal position of the Io footprint (Bonfond et al., 2009; Hess et al., 2010b). A new model of the Jovian internal magnetic field – called VIPAL – has been proposed (Hess et al., 2011a) to correct the VIP4 longitudinal inaccuracy by fitting the positions of the observed Io footprints as a function of the longitude of Io. This model may also better describe the magnetic field along the footpaths of Io as suggested by radio observations (Hess et al., 2011a). In the present study, we use both the VIP4 and VIPAL internal magnetic field models associated with the (Connerney et al., 1981) current sheet magnetic field model. These two models present close values and similar profiles of the magnetic field strength at Io, as shown in Panel (a) of Fig. 3.

The plasma torus is observable from Earth (e.g. Schneider and Trauger, 1995) and has been explored by the Voyager, Galileo and Ulysses spacecraft. These observations show that the Io torus is mostly composed of cold (a few tens of eV) ions derived from SO_2 dissociation and ionization. The plasma density varies around a characteristic density of $\sim$2000 cm^{-3} (Bagenal, 1994). The torus scale height is about 0.9R_J (Bagenal, 1994). Due to the different inclinations of Io's orbit and of the plasma torus plane, the angular distance between Io and the center of the torus varies as $\sim 7^\circ \cos(\lambda_{Io} - 20^\circ)$ (Schneider and Trauger, 1995), which corresponds to a maximum distance of $\sim 0.8 R_J$, comparable to the torus scale-height. Hence, the plasma density in the vicinity of Io varies with the longitude, as shown in Panel (b) of Fig. 3.

Panel (c) of Fig. 3 shows the modulation of the power generated at Io as a function of longitude, due to the magnetic field strength and density variation. The amplitude of this variation is about $\pm$ 18% of the mean value.

3. Power transmission along the magnetic field lines

3.1. Model of the Alfvén wave packet

The power transmission along the Io flux tube depends strongly on the Alfvén wavelengths (Hess et al., 2010a). The interaction of Io with the magnetosphere involves Alfvén waves with a characteristic perpendicular wavelength of the order of the satellite diameter, and a parallel wavelength of the order of the

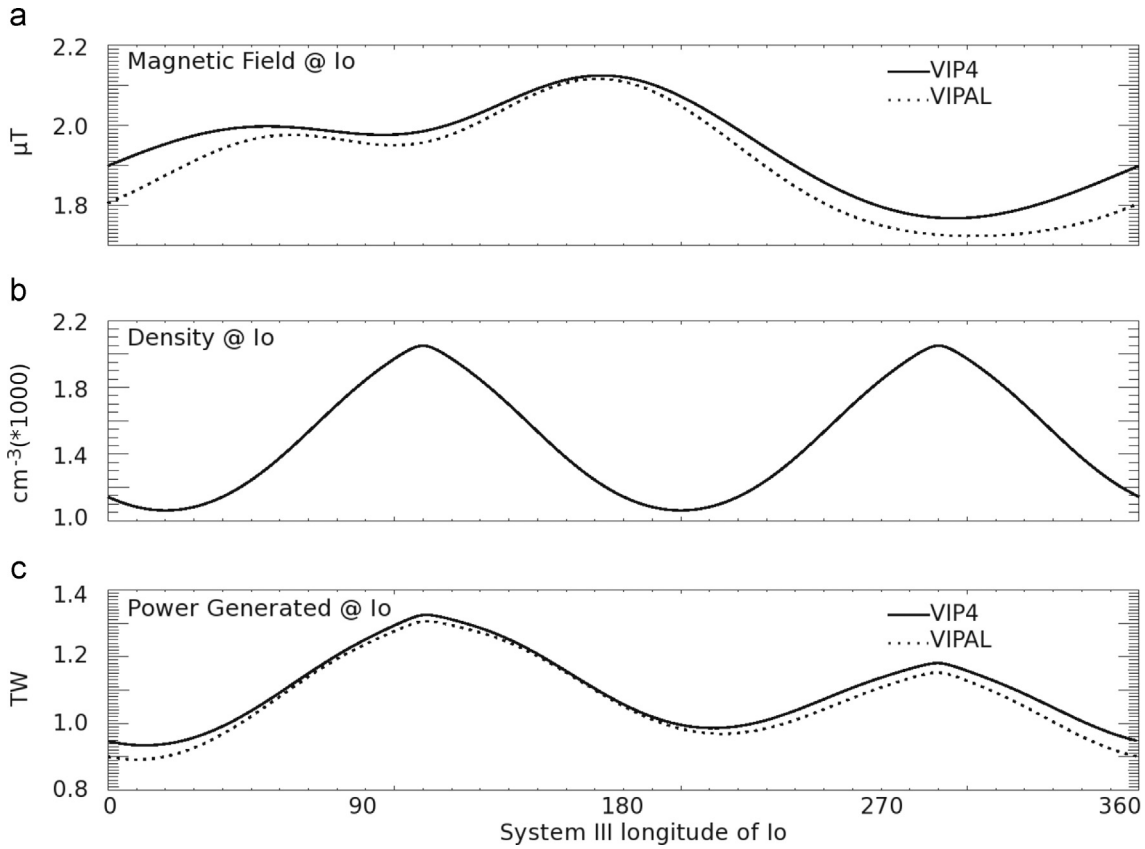

Fig. 3. Modulation of the magnetic field at Io (top), of the density at Io (middle) and of the power generated per hemisphere at Io (bottom) for both the VIP4 and VIPAL magnetic field models.

Alfvén wave speed close to Io multiplied by the duration of the interaction (i.e. a few Io diameters). While simple Gaussian distributions would be expected to describe well the Alfvén wave spectra, Hess et al. (2010a) showed that a power law distribution is required in order to be consistent with the observations. The authors proposed that the Alfvén wave may be filamented by the turbulence in the plasma close to Io. This is supported by the observations of short Alfvén wavelengths close to Io by the Galileo spacecraft (Chust et al., 2005). However, the turbulence near Io has not been studied so far.

We use a $k_{\perp}^{-2}$ spectrum for the Alfvén waves generated at Io. Such a spectrum has been observed in Saturn's magnetosphere by Cassini (Saur et al., 2002) and theoretical studies and simulations of the turbulence in strongly magnetized plasma suggest a similar spectral index value (Galtier et al., 2000; Galtier, 2009; Champeaux et al., 1998; Sharma et al., 2008, and references therein).

Theoretical studies predict spectral indices of the parallel wavevector distribution between $-5/2$ and $k_{\parallel} \sim k_{\perp}^{2/3}$ (i.e. spectral index of $-4/3$) (Galtier, 2009), depending on the assumption under which the calculation is performed. This range is rather large and the observations in Io's vicinity do not permit the measurement of the spectral index, nor constrain the required parameters to determine it theoretically. Hence, we assume a standard Kolmogorov spectrum for the parallel component ($k_{\parallel}^{-5/3}$) in the present study. This value is within the possible values allowed by the theoretical studies and is the most standard approximation of the spectral index of the perturbations in a turbulent plasma. Hess et al. (2011c) also considered $k_{\parallel}^{-2}$. The tests carried by these authors with both power law values resulted in similar variations, with the $k_{\parallel}^{-2}$ spectrum corresponding to aurorae slightly dimmer than with the Kolmogorov spectrum.

The power law is considered to be between an injection scale (k_0) and the dissipation (ionic) scale $k_i = \omega_p/(m_i c)$. For wavevectors smaller than k_0 and larger than k_i, we assume a Gaussian distribution with a half width k_0. The injection scale corresponds to the diameter of Io in the perpendicular direction and is equal to $V_a \tau$ in the parallel direction, where τ is the characteristic duration of the interaction (the time for a magnetic field line to pass Io, i.e. ~ 60 s).

3.2. Model of the power transmission

The electric current flowing through the satellites creates a deformation of the nearby magnetic field lines. This perturbation has the form of Alfvén waves carrying a current along the magnetic field lines toward the planetary ionosphere. The Alfvén waves encounter several changes in the plasma parameters (in particular at the plasma torus boundaries and near the planetary ionosphere), which cause the partial reflection of the wave packet due to strong variations of the Alfvén phase velocity ($V_{\phi,a}$).

The WKB and the discontinuity approximations provide much higher or much lower reflection coefficients to account for the observed brightnesses, respectively (Wright, 1987). These approximations differ in the ratio between the wavelength and the assumed characteristic scale of the phase velocity gradient (short and long wavelengths for the WBK and discontinuity approximations, respectively). The wavelength spectrum of the Alfvén waves generated by the satellite–planet interaction covers an intermediate range and cannot be described by the above approximations (Wright, 1987). In Hess et al. (2010a), the authors developed a new method to compute the reflection coefficient consistent with the WKB and the discontinuity approximations for short and long

wavelengths, respectively. In terms of spectral power carried by the Alfvén waves ($\mathcal{P}_w$), the reflection coefficient approximation is given by Hess et al. (2010a):

$$\frac{d\mathcal{P}_w}{ds}(s,\mathbf{k}) = \frac{-\mathcal{P}_w(s,\mathbf{k})}{\lambda_\parallel}\left(\int_{s-\frac{\lambda_\parallel}{2}}^{s+\frac{\lambda_\parallel}{2}} \frac{\nabla_s \ln(c/V_{\phi,a}(\mathbf{k}))}{2}\, ds\right)^2 \tag{4}$$

where s is the curvilinear distance along the magnetic field lines. Eq. (4) is explicitly dependent on the parallel wavelength ($\lambda_\parallel$). The dependence on the perpendicular wavelength occurs through the phase velocity ($V_{\phi,a}$) but can be neglected as $V_{\phi,a} \simeq V_a$ over most of the spectrum (Hess et al., 2010a). This equation implies that short wavelengths are weakly reflected whereas long wavelengths are strongly reflected. The overall reflection is then intermediate between the WKB and discontinuity approximations. The numerical integration of this equation allows us to define the transmission coefficient between Io and the acceleration region ($T(k_\parallel)$):

$$T(k_\parallel) = \frac{\mathcal{P}_w(s_{acc}, k_\parallel)}{\mathcal{P}_w(0, k_\parallel)} \tag{5}$$

where s_{acc} is the position of the acceleration region, defined as the peak location of the parallel electric field associated with the Alfvén wave (see next section). $G_\parallel$ stands for the ratio of the total (integrated over k) power reaching the acceleration region ($P_w(s_{acc})$) and that generated at Io ($P_w(0)$) :

$$G_\parallel = \frac{P_w(s_{acc})}{P_w(0)} = \int_0^\infty T(k_\parallel) f(k_\parallel)\, dk_\parallel. \tag{6}$$

Eq. (4) implies a non-negligible reflection outside of the torus boundaries, there large Aflvén velocities imply long parallel wavelengths. Indeed, the Alfvén phase velocity gradient is maximum near $1R_J$ from the torus center, but the velocity gradient outside of the torus remains significant.

Panel (a) of Fig. 4 shows the fraction of the power generated at Io which reaches the acceleration region ($G_\parallel$) computed for the northern and southern hemispheres with the VIP4 and VIPAL magnetic field models. Approximately 30% of the power generated at Io reaches the acceleration region. The amplitude of the modulation relative to the mean value is about 8–9% in the southern hemisphere, and 10–12% in the northern one.

The $G_\parallel$ coefficient does not directly depend on the position of Io in the torus as could intuitively be expected. Panel (b) of Fig. 4 shows the transmission coefficients as a function of the distance between Io and the reflecting torus border, i.e. the distance traveled by the Alfvén waves in the torus. The transmission coefficient tends to be lower when this distance is shorter, however a correlation is not evident.

Panel (c) of Fig. 4 shows that the transmission of the wave power is lower for larger Alfvén velocities at the reflecting torus border. The parallel Alfvén wavelengths are proportional to the Alfvén velocity. Hence, the parallel wavelengths of the Alfvén waves are shorter for low Alfvén velocities at the torus border (i.e. at the peak of the index gradient), implying a better transmission. The correlation between the distance traveled by the wave in the torus and the transmission coefficient can be attributed to the position of the torus in the centrifugal plane, between the magnetic equator (where the magnetic field tends to be lower) and the Jovigraphic equator (where Io orbits). As a consequence, the torus border farthest from Io is the closest to the magnetic equator and corresponds to lower magnetic fields, i.e. lower Alfvén velocities, and thus to a more effective power transmission.

4. Power transfer to the electrons

The parallel electric field generated by an inertial Alfvén wave can be approximated by Lysak and Song (2003):

$$\delta E_\parallel \simeq \omega_a k_\perp \lambda_e^2 \delta B \tag{7}$$

where ω_a is the Alfvén frequency, λ_e is the electron inertial length, $k_\perp$ the Alfvén perpendicular wavevector and δB the magnetic field perturbation associated with the wave. The amplitude profile of the parallel electric field along the magnetic field lines associated with the Alfvén waves has a narrow peak just above the Jovian ionosphere (i.e. at an altitude of $\sim 0.5R_J$), which likely is the cause of the electron acceleration (Hess et al., 2010a, 2011c). The localization of the electric field generates impulsive accelerations of the electrons, both toward Jupiter and in the antiplanetward direction. Numerical simulations show that the accelerated electrons have a "kappa-like" distribution in energy, i.e. a Gaussian core with the tail of the distribution described by a power law with a mean energy of a few keV (Swift, 2007; Hess et al., 2010a). Such distributions have been observed on the downstream side of Io (Frank and Paterson, 1999; Mauk et al., 2001; Williams et al., 1996, 1999; Williams and Thorne, 2003) and have been inferred from the altitude distribution of the UV footprint aurorae (Bonfond et al., 2009; Bonfond, 2010).

The power transferred to the electrons by an Alfvén wave packet can be estimated by assuming that, for each Alfvén wavelength, the electrons are accelerated by the parallel electric field associated with the Alfvén wave during a half-period of the wave. Hess et al. (2010a, 2011c) showed that in this case, an Alfvén wave carrying a power $P_w(s_{acc})$ transfers to the electrons a power P_e given by

$$H_\perp = \frac{P_e}{P_w(s_{acc})} = \int_0^\infty \min\left(\frac{\pi^2}{8}\frac{V_{th} k_{\perp;acc}^2 \lambda_e^2}{V_{\phi;a}(k_\perp)}; 1\right) f(k_\perp) dk_\perp \tag{8}$$

where $V_{\phi,a}(k_\perp)$ is the phase velocity of an Alfvén wave whose perpendicular wavenumber is $k_\perp$ in the equatorial plane and $k_{\perp;acc}$ in the acceleration region. Before their acceleration, the electrons have a thermal velocity V_{th} and an inertial length λ_e. $f(k_\perp)$ is the perpendicular wavenumber distribution of the Alfvén wave packet generated in the equatorial plane. One can separate the propagation effects ($G_\parallel$, which depends on $k_\parallel$) from the electron acceleration ($H_\perp$, which depends on $k_\perp$) to link the total power transferred to the electrons (P_e) to the total power generated at Io ($P_w(0)$) given by Eq. (3):

$$P_e = G_\parallel H_\perp P_w(0). \tag{9}$$

It is assumed that a given flux tube acts as a wave-guide for the Alfvén waves. As the magnetic field lines converge toward the planet, the cross-section of the flux tube decreases, implying an increase of the perpendicular wavevector. In most of the theoretical studies the flux tube cross-section is assumed to be circular. In this case, the perpendicular wavevector in the acceleration region is related to the perpendicular wavevector in the equatorial plane by

$$k_{\perp;acc} = \sqrt{\mu_{acc}} k_\perp. \tag{10}$$

The μ_{acc} term is the mirror ratio, i.e the magnetic flux ratio between the acceleration region and the equatorial plane. Assuming that the flux tube cross-section is always circular is probably erroneous as the magnetic field convergence is not the same in the longitudinal and latitudinal directions (Bonfond, 2010). The current carrying fluxtube may not even be circular in the equatorial plane as the magnetic field line perturbation may be more extended along Io's wake than perpendicular to it. We note χ_λ the ratio between the wavevector along the Io footpath in the Jovian ionosphere and the wavevector along the Io orbit in the

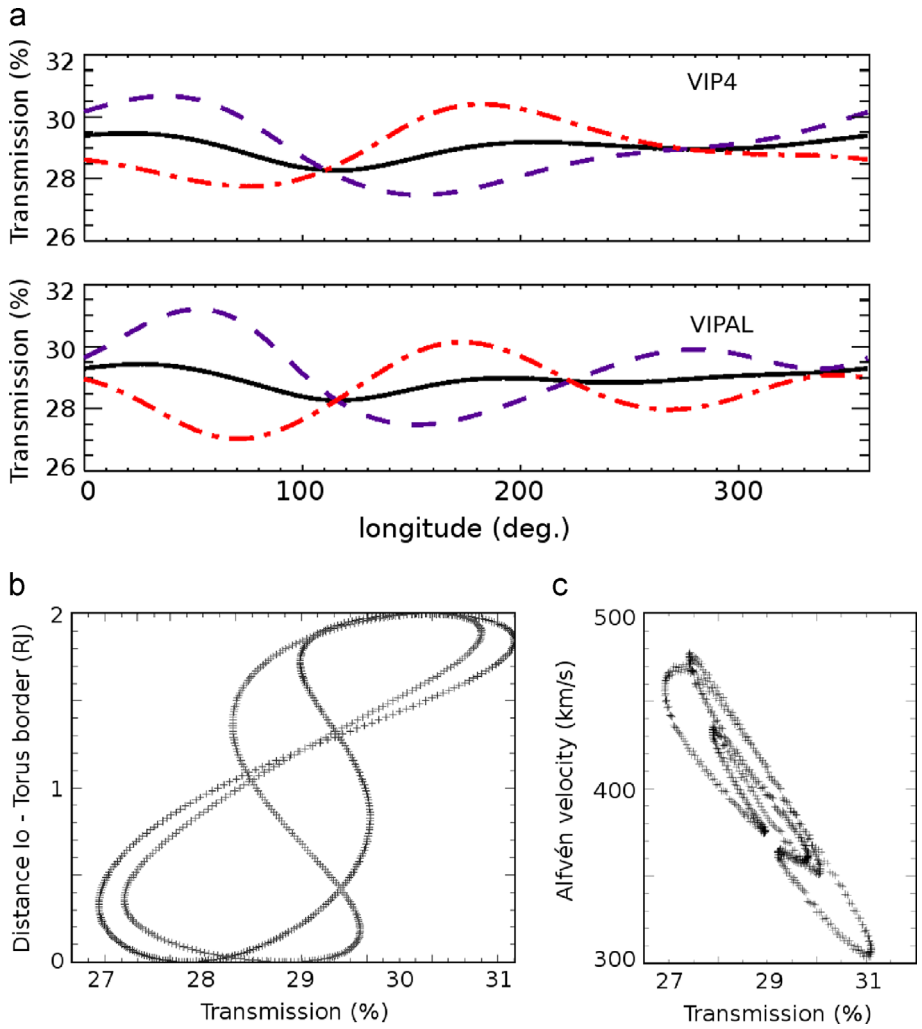

Fig. 4. (a) Modulation of the Alfvén wave transmission to the acceleration region in the Northern (dashed) and Southern (dash-dotted) hemispheres, versus the System III longitude of Io. The solid line represents the hemispheric average. The computation has been performed for the VIP4 and VIPAL magnetic field models. (b) Transmission as a function of the distance between Io and the reflecting torus border. (c) Transmission as a function of the Alfvén velocity at the reflecting torus border. The torus border position is set to a distance of $1R_J$ from the torus center.

equatorial plane, and $\chi_\perp$ the ratio between the wavevectors perpendicular to it in the ionosphere and equatorial plane. The conservation of the magnetic flux across the flux tube cross-sections imposes

$$\mu_{acc} = \chi_\lambda \chi_\perp . \tag{11}$$

In the following, we simulate the circular flux tube case and a fluxtube much more extended along the direction of Io's orbit than along the perpendicular direction. In this latter case, the perpendicular wavevector in the acceleration region is related to the perpendicular wavevector in the equatorial plane by

$$k_{\perp;acc} \simeq \chi_\perp k_\perp . \tag{12}$$

Fig. 5 shows the efficiency of the power transfer to the electrons for the VIP4 and VIPAL magnetic field models under the assumption of an Io flux tube with either a circular cross-section or an infinite extension along Io's orbit. For both magnetic field models, the variation is larger when an Io flux tube with an infinite extension along Io's orbit is assumed. The amplitude of the modulation relative to the mean is $\sim 9\%$ for the VIP4-circular fluxtube case, whereas the northern and southern amplitudes reach 50% and 36%, respectively, for the VIPAL-elongated fluxtube scenario. For the two other cases, the amplitude ranges between 15% and 25% depending on the hemispheres.

5. Modulation of the precipited power

5.1. Main Alfvén wing spot

The power carried by the electrons accelerated toward Jupiter may be obtained using Eq. (9). Still, between the acceleration region and the aurorae location, the magnetic field dramatically increases. This results in the magnetic mirroring of the accelerated electrons, which varies with longitude. Magnetic mirroring reflects electrons if their velocity is such that $V_\perp/V > \sqrt{B/B_{surface}}$. The power lost by magnetic mirroring depends on the electron velocity distribution.

Alfvén waves accelerate electrons along the magnetic field in such a way that they acquire a kappa distribution in this direction (Swift, 2007; Bonfond et al., 2009). The perpendicular velocity remains unchanged in first approximation. We model the accelerated electron distribution as a Gaussian with a temperature of 100 eV in the perpendicular direction, and a Kappa with a kinetic temperature of 100 eV and a mean energy of 1 keV in the parallel direction (consistent with Bonfond et al., 2009). Fig. 6 shows the fraction of the power carried by the electrons accelerated toward the main spots (north and south) which is not reflected by magnetic mirroring, depending on the magnetic field model. The amplitude of the modulation corresponds to $\pm$ 9% of the mean

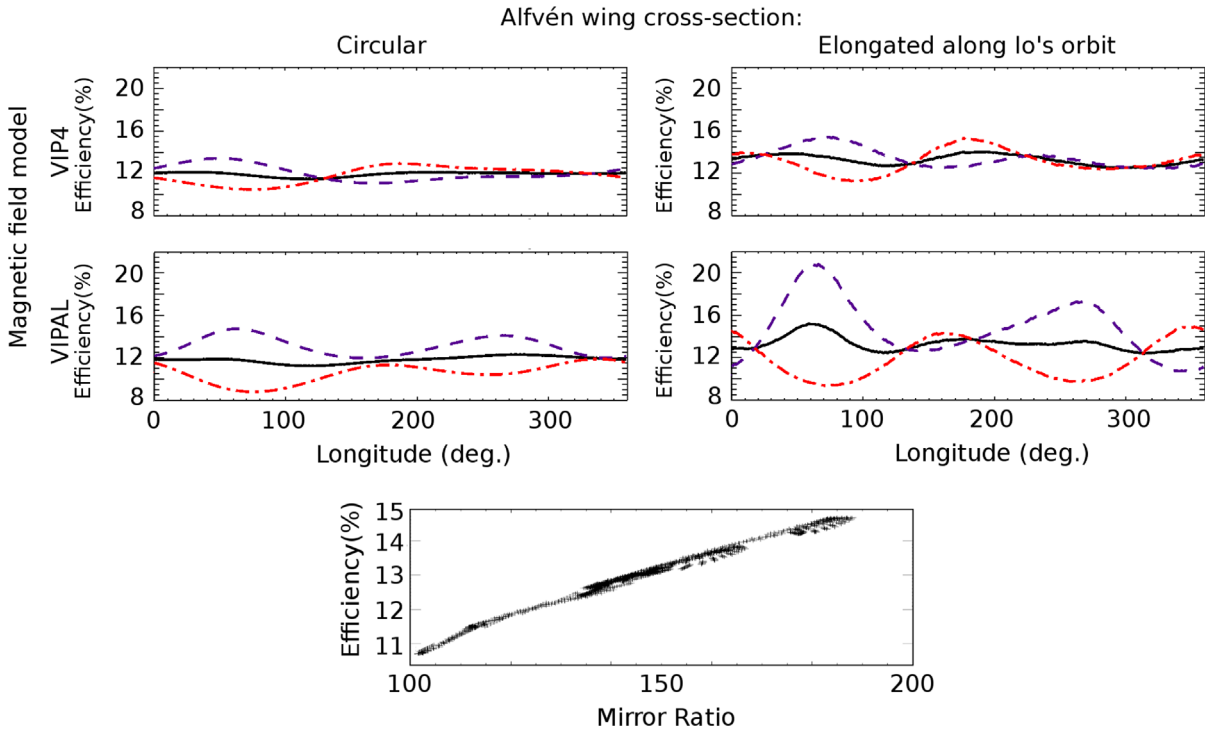

Fig. 5. (a) Modulation of the power transfer to the electrons in the Northern (dashed) and Southern (dash-dotted) hemispheres, versus the System III longitude of Io. The computation has been performed for the VIP4 and VIPAL magnetic field models, and for a IFT cross-section circular and elongated along the orbit of Io. The solid line represents the hemispheric average. (b) Dependence of the efficiency of the power transfer to the electrons on the mirror ratio μ_{acc}, computed for the models with a circular IFT cross-section.

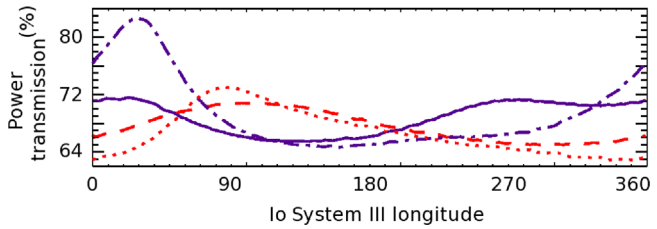

Fig. 6. Fraction of the electron beam power which is not magnetically mirrored between the acceleration region and the surface of the planet. Solid and dashed lines stand for northern and southern hemispheres computed with the VIP4 model, respectively. Dash-dotted and dotted lines stand for northern and southern hemispheres computed with the VIPAL model, respectively.

value for VIP4. It reaches ~25% (north) and ~15% (south) for VIPAL.

To compare the models and observations, we chose to convert the precipitated powers predicted by the models and the observed brightnesses into energy fluxes precipitated into Jupiter's atmosphere. Indeed the models assume a certain size of the interaction region (namely the size of Io), whereas the extent of the auroral spots corresponds to a much more extended region of interaction along the orbit of Io. The size of the spots used to fit the observations is fixed and constant, so we convert the power obtained from the models to energy fluxes using the averaged surface of Io projected on each hemisphere. This way, we do not introduce different biases for the observations and the models.

Figs. 1 and 2 show the energy flux precipitated on the Io main spots versus the longitude when magnetic mirroring is taken into account in the northern and southern hemisphere, respectively. These profiles are superimposed on the observations. We reproduce well the slow low-amplitude modulation of the main spots. The southern MAW energy flux is correctly estimated by our model (with the exception of the peak near 110°), but the northern MAW spot energy flux is overestimated by a factor of ~2.

5.2. Transhemispheric electron beams spot

Electrons accelerated by Alfvén waves are directed both toward the planet and anti-planetward, because the sign of the parallel electric field depends on the phase of the wave, which changes with time and location. Hence, at the same time when electrons are accelerated toward Jupiter above the main spots, part of the electron distribution is also accelerated in the opposite direction and precipitated in the opposite hemisphere after crossing the torus.

The Alfvén waves propagate slowly in the Io torus over different distances toward north and south, introducing a delay (and thus a longitudinal shift) between the generation of the northern and southern MAW spots. In comparison, the time needed by keV electrons to travel from one hemisphere to the other is negligible (<30 s). Therefore, the electrons accelerated anti-planetward do not precipitate on the conjugate main (MAW) spot, but create a spot of their own (Bonfond et al., 2008) called TEB (transhemispheric electron beams) spot.

The powers of the electrons accelerated anti-planetward and planetward are the same, but the MAW and conjugate TEB spots do not receive the same amount of power, for two reasons: the loss by magnetic mirroring is different between hemispheres, and part of the electrons may be intercepted by Io or lost in the torus. This last point is supported by the observation of electron beams above Io's poles (Williams and Thorne, 2003); by models (Jacobsen et al., 2010); and by the altitudinal profile of the TEB spots (Bonfond, 2010). The TEB spot is emitted deeper in the Jovian ionosphere and with a smaller altitudinal extention than the other spots. This suggests that the distribution of the transhemispheric electron beams is depleted in electrons with energies lower than a

few keV, which is consistent with loss by collision of low energy electrons in the cold torus. This certainly varies with the position of Io in the torus, but describing it correctly requires an accurate simulation of the plasma kinetics along the whole Alfvén wing – including Io's vicinity – which is beyond the scope of the present paper. Thus, we assume a constant loss. Since about half of the power of the accelerated electrons is due to electrons with energies lower than a few keVs, we set the loss of power of the electron beams crossing the torus to 50%.

Part of the particles magnetically mirrored between the acceleration region and the MAW spot will join the transhemispheric electrons. These electrons are included in the present study, taking into account the difference of the magnetic mirror ratios between the two hemispheres.

Figs. 1 and 2 show the power precipitated on the TEB spots in the northern and southern hemispheres, respectively. The same four cases as for MAW spots are considered (VIP4/VIPAL, circular/elongated cross-sections). The brightness value and variation are consistent with the observations, even though they do not reproduce them perfectly. This discrepancy is expected as we do not model accurately the loss of power in the torus. Since we lack constraints for the loss of power in the torus, an adjustment of the coefficients for a better correlation with the observations would be completely arbitrary. The southern hemisphere TEB spot may receive more power than the MAW spot between $\sim 60^\circ$ and $\sim 90^\circ$, depending on the models.

5.3. Reflected Alfvén wing spot

Part of the Alfvén wing is reflected on the torus border, generating reflected Alfvén wings in the torus, which behave similarly to the main Alfvén wing. Thus, the reflected Alfvén wings generate spots, called the RAW (reflected Alfvén wing) spots. We compute the power precipitated on the first of these RAW spots (corresponding to a single reflection) the same way we computed the power precipitated on the MAW spot. The only difference is that a primary reflection coefficient must be added in Eq. (9), which becomes

$$G'_{\parallel} = \int_0^{\infty} T(k_{\parallel}) R_{conj}(k_{\parallel}) (f(k_{\parallel})\, dk_{\parallel} \tag{13}$$

with R_{conj}, the reflection coefficient of the wave at the torus border in the opposite hemisphere, computed by integrating Eq. (4) between Io's position and a distance of $2R_J$ from the torus center in the opposite hemisphere ($2R_J$ being roughly twice the torus scale-height):

$$R_{conj}(k_{\parallel}) = \frac{\mathcal{P}_w(-2R_J, k_{\parallel})}{\mathcal{P}_w(0, k_{\parallel})} \tag{14}$$

The reflection on the torus border R_{conj} represents only half of the reflections occurring between Io and the acceleration region, meaning that half of the power loss in the Alfvén wing takes place between the torus border and the acceleration region. This is due to the increase of the magnetic field (V_a gets multiplied by 5 to 10) in a region where the parallel Alfvén wavelength is large (since $V_a > 0.1$ c). The Alfvén waves reflected out of the torus are partly trapped between the torus border and the Jovian ionosphere, and contribute to the generation of the diffuse tail. Radio emissions in the decameter range show traces of this trapping in the form of arcs echoing the main radio arc (Queinnec and Zarka, 1998).

Figs. 1 and 2 show the power precipitated on the RAW spots in the northern and southern hemispheres, respectively, for the two magnetic field models and the two flux tube cross-sections simulated. The mean value of the energy flux is consistent with the observations.

6. Comparison with observations

6.1. Mean values and slow modulation

Both observations and modeling are summarized in Figs. 1 and 2 which show the energy fluxes precipitating above the Io spots, in the northern and southern hemispheres respectively. On these figures, blue, green and red colors stand for the MAW, RAW and TEB spots, respectively. Crosses stand for energy fluxes deduced from the observed brightnesses, whereas lines stand for the modeled energy fluxes.

All four models of Fig. 2 (standing for the southern hemisphere) are similar, even if the VIPAL+elongated flux tube scenario gives larger variations, and are in good agreement with the observation, except for longitudes of Io between 80° and 140°. At these longitudes, there is a peak in the observed energy fluxes which is discussed in the next section. In the remaining longitude range, the energy fluxes on top of the MAW spot are fitted with a deviation much smaller than the dispersion of the measurements.

In the same figure, the averaged values of the energy fluxes on top of the TEB and RAW spots (excluding the 110° region) are in good agreement with the observations, although the models often predict slightly larger fluxes than observed. For the TEB spots, that may mean that the 50% loss we set for the electron beams crossing the torus is not sufficient. However, as we cannot sufficiently constrain this value, we do not try to improve the fit of the observations. As far as the RAW spot is concerned, we find the worst agreement at longitudes near 200°. This region corresponds to a longitude range at which the RAW spot is supposed to have a low brightness according to the models and is at its closest distance from the brighter MAW spot (Bonfond et al., 2009). Hence, the discrepancy may originate from the weakness of this spots, which prevents from a precise estimate of its power. For longitudes of Io between 250° and 30°, the distribution of the TEB energy fluxes is bimodal, with a component close to 0 W/m^2 corresponding to observations where the background brightness is close to that of the TEB spot, in which case the TEB brightness may be poorly determined.

The variations of the TEB and MAW spots' brightnesses are in rough agreement with the data. For example, the maxima and the minima of the energy fluxes match those of the observations quite well. The TEB energy flux modulation predicted by the 'VIPAL+elongated fluxtubes' scenario is in particularly good agreement with the data, with the amplitude of the modulation being close to that observed. Moreover, the model predicts a peak of brightness for the TEB for longitudes close to 75° which is observed in the data (before it merges with the 110° peak which is not reproduced by any of our modelings).

Fig. 1 shows the same comparison for northern spots. All of the above comments also apply for the northern hemisphere, with the exception that all of the predicted energy fluxes are overestimated by a factor of ~ 2. This apparent weakness of the northern emissions when compared to southern ones cannot be explained by our model. The fact that it affects all the spots in the northern hemisphere (AWs and TEB) and none in the southern one implies that it cannot be related to a smaller power transfer to the electrons in the northern hemisphere (otherwise the modeled northern TEB would fit the data, whereas the modeled southern TEB would be twice brighter than observed). A modification of the magnetic mirroring through changes of the altitude of the acceleration region would have similar effects. Actually, there is no way to adjust our model to reproduce this feature, which means that some physics responsible for dimmer emissions in the northern hemisphere is absent from our model and thus requires further investigations. The amplitude of this effect appears to be independent from the longitude, despite the lack of a full longitudinal coverage of the northern hemisphere.

An interesting feature of the northern TEB spot predicted by the model is that its brightness does not vary as much as the southern one. The reason for this is that the mirror ratios between the northern and southern hemispheres reinforce the modulation of the TEB due to the other phenomena (reflection, acceleration, etc.) in the southern hemisphere, yet reduce these modulations in the northern one.

6.2. Peak at 110°

An interesting difference between our simulated MAW power profiles (Fig. 2) and the observed ones is the absence of the large peak when Io is at a longitude close to $\lambda_{Io} = 110°$ in our model. The main reason is that the observed peak is ~ 5 times higher than the minimum value and has a half-width of about 20°. None of the key parameters in the Jovian ionosphere (e.g. density and magnetic field) vary with such an amplitude or over such a short longitude range.

An explanation would be the merging of the TEB and MAW spots, which happen to have the same longitude when the System III longitude of Io is 110°. However, the fit of the observations in Paper I shows that both TEB and MAW spots peak near 110°. Hence, the peak of the MAW spot brightness cannot be interpreted as the result of a confusion between the MAW and the TEB spots as they begin to merge (in which case the TEB spot brightness would appear dimmer). A more decisive argument is that the southern RAW spot shows also a peak in brightness, although this spot is located farthest from the TEB and MAW for this longitude of Io. The only way to have those three spots peaking at the same time is to have a peak in the power generation at Io (as their current systems never mix again once they leave the satellite). This is also supported by the abrupt increase of the northern MAW spot brightness below 150° (even if there are no measurements for a longitude of Io of 110°).

Following Eq. (3), abrupt changes in the equatorial density and/or magnetic field can cause such a peak in the generated power, but they were never observed and would require such complex physics that they are very unlikely. Another phenomenon must take place at this particular longitude. Io is at the center of the torus at this longitude and Dols et al. (2008) showed that in this case, nearly 50% of the power is due to the momentum loading of the magnetic field lines around Io provided by the charge exchange between the torus ions and the Iogenic neutrals. Indeed, the current generated by these charge exchanges is proportional to the torus density, at least as a first approximation (Dols, personal communication). Moreover, Jacobsen et al. (2007) showed that a larger slowdown of the plasma flow also leads to non-linearities in the Alfvén wave generation and propagation, which ends up increasing the intensity of the current. However, Io is also in the center of the torus near a longitude of 290°, without generating such a huge peak of brightness in the auroral footprints, although Steffl et al. (2008) and Hess et al. (2011b) showed that on average the torus density is higher at a longitude of 290° than at a longitude of 110°.

A clue may be given by the present study. TEB spots from both hemispheres reach their maximum brightness near a longitude of Io of 90° and are still intense when Io reaches a longitude of 110°. At this longitude, northern and southern Alfvén wings become symmetric and the transhemispheric electron beams from northern and southern hemispheres are located on the same magnetic field lines. For a longitude of Io of 110° the "energetic" (i.e. accelerated) electron content of the flux tube in Io's wake reaches a maximum. At 290° both transhemispheric electron fluxes are much (almost twice) lower. Based on modeling and Galileo measurements, Dols et al. (2008) concluded that the "energetic" electron flux induces enhanced plasma ionization in Io's wake. This supplementary ionization leads to extra mass loading of the magnetic field line, and thus to a more intense interaction. Moreover, the part of the electron beam precipitating on Io increases the conductivity of Io's ionosphere, which leads in turn to a more effective deceleration of the plasma and results in non-linear effects and a stronger draping of the field line, as simulated by Jacobsen et al. (2007). Quantifying all the effects generated by the electron beams, including all the feedbacks, would require kinetic simulations, which are outside the scope of the present paper.

7. Conclusion

In the present study, we modeled the power transfer between the local magnetosphere interaction at Io and the UV emissions, based on our current knowledge of the interaction (Hess et al., 2010a). This modeling was performed for different longitudes of Io in order to investigate the modulation of the brightnesses of the Io spots. We succeeded in explaining the average brightness of the spots, even though we could not match exactly the brightness of the northern spots which are about half as bright as the southern ones. This asymmetry is still under investigation and no explanations for it have been proposed yet. Still, the relative brightness of the different spots in each hemisphere is correctly predicted, despite the approximations we had to make to perform the computations.

We also successfully reproduced the slow amplitude variations of the spots' brightness, i.e. excluding the peak of brightness for Io's System III longitudes close to 110°. However, our approach gives some clues toward an explanation of this feature. The modeling of the slow longitudinal modulation of the spots' brightness allowed us to explore the details of the satellite–magnetosphere interactions and to estimate more precisely the relative importance of the phenomena participating to the interaction and their sensitivity to the various plasma parameters.

The phenomena contributing the most to the variability of the spot brightness are the local interaction at Io (i.e. due to the variations of density and magnetic field close to Io) and the modulation of the efficiency of the power transfer to the electrons. Both vary by $\sim$ 20% relative to their mean value. The variation of the power transfer to the electrons may even reach 50% in some cases. The transmission of the Alfvén wave power through the torus varies by only 10% for the MAW spots. However, its contribution is larger (almost twice) for the reflected Alfvén wing spots. Finally, the mirroring of the electrons contributes from 10% to 20% to the brightness modulation of the spots.

The present study demonstrates the complexity of the satellite–magnetosphere interactions, with many phenomena acting at the same time and in different parts of the disturbed flux tubes. Every one of them has to be accounted for in order to obtain a consistent description of the interaction region. The study also suggests that these phenomena may be coupled through a feedback of the accelerated electrons on the local interaction in Io's vicinity.

Acknowledgments

The authors thank the reviewers for their careful and valuable reviews.

References

Bagenal, F., 1994. Empirical model of the Io plasma torus: Voyager measurements. Journal of Geophysical Research 99, 11043–11062.
Bagenal, F., 1997. Ionization source near Io from Galileo wake data. Geophysical Research Letters 24, 2111.

Bonfond, B., 2010. The 3-D extent of the Io UV footprint on Jupiter. Journal of Geophysical Research 115, A09217.
Bonfond, B., Grodent, D., Gérard, J., Radioti, A., Saur, J., Jacobsen, S., 2008. UV Io footprint leading spot: a key feature for understanding the UV Io footprint multiplicity?. Geophysical Research Letters 35, L05107.
Bonfond, B., Grodent, D., Gérard, J.C., Radioti, A., Dols, V., Delamere, P.A., Clarke, J.T., 2009. The Io UV footprint: location, inter-spot distances and tail vertical extent. Journal of Geophysical Research 114, A07224.
Bonfond, B., Hess, S.L.G., Grodent, D., Gérard, J.C., Radioti, A., Chantry, V., Saur, J., Jacobsen, S., Clarke, J.T. Evolution of the IFP brightness I: observations. Planetary and Space Sciences, in this issue. http://dx.doi.org/10.1016/j.pss.2013.05.023.
Branduardi-Raymont, G., Elsner, R.F., Galand, M., Grodent, D., Cravens, T.E., Ford, P., Gladstone, G.R., Waite, J.H., 2008. Spectral morphology of the X-ray emission from Jupiter's aurorae. Journal of Geophysical Research 113, A02202.
Champeaux, S., Passot, T., Sulem, P.L., 1998. Transverse collapse of Alfvén wave-trains with small dispersion. Physics of Plasmas 5, 100–111.
Chust, T., Roux, A., Kurth, W.S., Gurnett, D.A., Kivelson, M.G., Khurana, K.K., 2005. Are Io's Alfvén wings filamented? Galileo observations. Planetary and Space Science 53, 395–412.
Clarke, J.T., Ajello, J., Ballester, G., Ben Jaffel, L., Connerney, J., Gérard, J.C., Gladstone, G.R., Grodent, D., Pryor, W., Trauger, J., Waite, J.H., 2002. Ultraviolet emissions from the magnetic footprints of Io, Ganymede and Europa on Jupiter. Nature 415, 997–1000.
Clarke, J.T., Ballester, G.E., Trauger, J., Evans, R., Connerney, J.E.P., Stapelfeldt, K., Crisp, D., Feldman, P.D., Burrows, C.J., Casertano, S., Gallagher Jr., J.S., Griffiths, R. E., Hester, J.J., Hoessel, J.G., Holtzman, J.A., Krist, J.E., Meadows, V., Mould, J.R., Scowen, P.A., Watson, A.M., Westphal, J.A., 1996. Far-Ultraviolet Imaging of Jupiter's Aurora and the Io "Footprint". Science 274, 404–409.
Connerney, J.E.P., Acuña, M.H., Ness, N.F., Satoh, T., 1998. New models of Jupiter's magnetic field constrained by the Io flux tube footprint. Journal of Geophysical Research 103, 11929–11940.
Connerney, J.E.P., Acuna, M.H., Ness, N.F., 1981. Modeling the Jovian current sheet and inner magnetosphere. Journal of Geophysical Research 86, 8370–8384.
Connerney, J.E.P., Baron, R., Satoh, T., Owen, T., 1993. Images of excited H_3^+ at the foot of the Io flux tube in Jupiter's atmosphere. Science 262, 1035–1038.
Dols, V., Delamere, P.A., Bagenal, F., 2008. A multispecies chemistry model of Io's local interaction with the Plasma Torus. Journal of Geophysical Research 113, A09208.
Frank, L.A., Paterson, W.R., 1999. Intense electron beams observed at Io with the Galileo spacecraft. Journal of Geophysical Research 104, 28657–28670.
Galtier, S., 2009. Wave turbulence in magnetized plasmas. Nonlinear Processes in Geophysics 16, 83–98.
Galtier, S., Nazarenko, S.V., Newell, A.C., Pouquet, A., 2000. A weak turbulence theory for incompressible magnetohydrodynamics. Journal of Plasma Physics 63, 447–488.
Gérard, J.C., Gustin, A., Grodent, D., Delamere, P., Clarke, J.T., 2006. Excitation of the FUV Io tail on Jupiter: characterization of the electron precipitation. Journal of Geophysical Research 107, SMP 30-1.
Gérard, J.C., Saglam, A., Grodent, D., Clarke, J.T., 2006. Morphology of the ultraviolet Io footprint emission and its control by Io's location. Journal of Geophysical Research 111, A12210.
Goertz, C.K., 1983. The Io-control of Jupiter's decametric radiation – the Alfven wave model. Advances in Space Research 3, 59–70.
Goldreich, P., Lynden-Bell, D., 1969. Io, a Jovian unipolar inductor. Astrophysical Journal 156, 59–78.
Gurnett, D.A., Goertz, C.K., 1981. Multiple Alfven wave reflections excited by Io origin of the Jovian decametric arcs. Journal of Geophysical Research 86, 717–722.
Hess, S.L.G., Bonfond, B., Zarka, P., Grodent, D., 2011a. Model of the Jovian magnetic field topology constrained by the Io auroral emissions. Journal of Geophysical Research 116, A05217.
Hess, S.L.G., Delamere, P., Dols, V., Bonfond, B., Swift, D., 2010a. Power transmission and particle acceleration along the Io flux tube. Journal of Geophysical Research 115, A06205.
Hess, S.L.G., Delamere, P.A., Bagenal, F., Schneider, N., Steffl, A.J., 2011b. Longitudinal modulation of hot electrons in the Io plasma torus. Journal of Geophysical Research 116, 11215.
Hess, S.L.G., Delamere, P.A., Dols, V., Ray, L.C., 2011c. Comparative study of the power transferred from satellite-magnetosphere interactions to auroral emissions. Journal of Geophysical Research 116, A01202.
Hess, S.L.G., Petin, A., Zarka, P., Bonfond, B., Cecconi, B., 2010b. Lead angles and emitting electron energies of Io-controlled decameter radio arcs. Planetary and Space Sciences 58, 1188–1198.
Jacobsen, S., Neubauer, F.M., Saur, J., Schilling, N., 2007. Io's nonlinear MHD-wave field in the heterogeneous Jovian magnetosphere. Geophysical Research Letters 34, L10202.
Jacobsen, S., Saur, J., Neubauer, F.M., Bonfond, B., Gérard, J.C., Grodent, D., 2010. Location and spatial shape of electron beams in Io's wake. Journal of Geophysical Research (Space Physics) 115, 4205.
Lysak, R.L., Song, Y., 2003. Kinetic theory of the Alfvén wave acceleration of auroral electrons. Journal of Geophysical Research 108, 1–6.
Mauk, B.H., Williams, D.J., Eviatar, A., 2001. Understanding Io's space environment interaction: recent energetic electron measurements from Galileo. Journal of Geophysical Research 106, 26195–26208.
Neubauer, F.M., 1980. Nonlinear standing Alfven wave current system at Io – theory. Journal of Geophysical Research 85, 1171–1178.
Prangé, R., Rego, D., Southwood, D., Zarka, P., Miller, S., Ip, W., 1996. Rapid energy dissipation and variability of the Io–Jupiter electrodynamic circuit. Nature 379, 323–325.
Queinnec, J., Zarka, P., 1998. Io-controlled decameter arcs and Io–Jupiter interaction. Journal of Geophysical Research 103, 26649–26666.
Saur, J., Politano, H., Pouquet, A., Matthaeus, W.H., 2002. Evidence for weak MHD turbulence in the middle magnetosphere of Jupiter. Astronomy and Astrophysics 386, 699–708.
Saur, J., Strobel, D.F., Neubauer, F.M., Summers, M.E., 2003. The ion mass loading rate at Io. Icarus 163, 456–468.
Schneider, N.M., Trauger, J.T., 1995. The structure of the Io torus. Astrophysical Journal 450, 450–462.
Serio, A.W., Clarke, J.T., 2008. The variation of Io's auroral footprint brightness with the location of Io in the plasma torus. Icarus 197, 368–374.
Sharma, R.P., Kumar, S., Singh, H.D., 2008. Nonlinear evolution of kinetic Alfvén waves and the turbulent spectra. Physics of Plasmas 15, 082902–082911.
Steffl, A.J., Delamere, P.A., Bagenal, F., 2008. Cassini UVIS observations of the Io plasma torus. IV. Modeling temporal and azimuthal variability. Icarus 194, 153–165.
Swift, D.W., 2007. Simulation of auroral electron acceleration by inertial Alfvén waves. Journal of Geophysical Research 112, A12207.
Thomas, N., Bagenal, F., Hill, T.W., Wilson, J.K., 2004. The Io neutral clouds and plasma torus. In: Jupiter. The Planet, Satellites and Magnetosphere, pp. 561–591.
Wannawichian, S., Clarke, J.T., Nichols, J.D., 2010. Ten years of Hubble Space Telescope observations of the variation of the Jovian satellites' auroral footprint brightness. Journal of Geophysical Research 115, A02206.
Williams, D.J., Mauk, B.H., McEntire, R.E., Roelof, E.C., Armstrong, T.P., Wilken, B., Roederer, J.G., Krimigis, S.M., Fritz, T.A., Lanzerotti, L.J., 1996. Electron beams and ion composition measured at Io and in its torus. Science 274, 401–403.
Williams, D.J., Thorne, R.M., 2003. Energetic particles over Io's polar caps. Journal of Geophysical Research 108, 1397.
Williams, D.J., Thorne, R.M., Mauk, B., 1999. Energetic electron beams and trapped electrons at Io. Journal of Geophysical Research 104, 14739–14754.
Wright, A.N., 1987. The interaction of Io's Alfven waves with the Jovian magnetosphere. Journal of Geophysical Research 92, 9963–9970.